Using WIPL-D EM Simulation to Prepare a W2IMU Feedhorn for a 0.5 f/D Offset Dish and Adapt to WR22 at 47 GHz

Oliver Barrett KB6BA

ABSTRACT

My 47 GHz radio project motivated me to apply electromagnetic (EM) simulation to a suitable feedhorn for it, with the hope that my experience with the WIPL-D software package will also be of practical interest to microwave hams. Selecting the W2IMU dual mode feedhorn design, I wanted to 1) double-check the mechanical dimensions needed for good performance using my 0.5 f/D offset dish before feedhorn fabrication, 2) improve the coupling to WR22 waveguide and 3) build my EM simulation expertise for microwave work in general. In this project, my WIPL-D and Phasepat simulation verified the W2IMU feedhorn performance at 47 GHz as having a 76.5 % peak efficiency at an f/D of 0.58 (74 % at 0.5), for a 1.30 wavelength output aperture. I used the WIPL-D EM software to construct the feedhorn along the lines of the G0IVA model, with the addition of a quarter-wave circular-to-rectangular transition plate, and performed simulations to determine the effect of varying output aperture length (and corresponding diameter and flare half-angle) for f/D values closer to 0.5. The simulations also showed the effect of good phase center selection on efficiency at smaller apertures. -23.0 dB return loss was achieved in the fabricated feedhorn. The WIPL-D software was found to be very capable of easily modeling complex shapes in the feedhorn design and being able to show the effects of dimensional changes quickly, yet exhibiting robust stability in the Windows 10 platform.

I. Introduction

After operating for a few years on 10 and 24 GHz, my interest centered on building a radio for 47 GHz. A crucial component is the feedhorn to be used at the focus of my offset dish, which has an f/D ratio of 0.5. I studied Paul Wade's discussion of several feedhorns based on the dual mode W2IMU design in his Antenna Book Online[1]. I came across a machined feedhorn there for 47 GHz by David Woodward, G0IVA[2], and set about using that for my dish with a couple of modifications in mind.

I had been interested in playing with electromagnetic (EM) simulation software for a long time, and this project provided an ideal opportunity to apply it. My goal was to not only verify the expected satisfactory performance, but also to see if I could better tailor the design to my system before committing the design to the machine shop (I don't have lathe or milling expertise), and by so doing, establish the practicality of WIPL-D for ham microwave applications as a modern alternative to NEC2.

In this paper, I describe how I accomplished that goal. Section II lists the important features of the W2IMU design, one of which is the choice of output aperture diameter. Section III lists some EM simulation software choices available on the market. Almost all of the ones I found are extremely expensive, both to purchase and to rent, with three exceptions. I describe why I chose WIPL-D[3] for this project. Many of these software packages use the Method of Moments mathematical theory, whose basic features are described in Section IV.

I then dive into the simulations, starting first with a simple waveguide termination to illustrate the WIPL-D environment in section V. My intent in this paper is to illustrate the utility of this software for microwave experimenters, but space does not permit a tutorial approach.

Construction and simulation of the feedhorn itself is shown in Sections VI and VII. I take advantage of the fact that key dimensions can be represented as variables that can easily be changed, and also that the meshing density used to preserve simulation accuracy is adjustable via a parameter "n". A key software feature is its ability to simulate the return loss as viewed at the reference plane located at the actual feedhorn entry point, even though a probe wire and short section of rectangular waveguide (not present in the actual machined feedhorn) are used to excite it. This de-embedding process can be thought of as the waveguide analog to VNA cable nulling.

Also discussed is how a quarter-wave waveguide transition plate was added to optimize the return loss, along with how I varied the output aperture diameter (and the corresponding output section length and flare half-angle) to see what would happen to the peak efficiency curve as it shifted towards the 0.5 f/D point, using one phase center value estimated from the WIPL-D phase data and a second value obtained from Paul Wade's Phasepat program, which also calculated the feedhorn efficiency curves.

The return loss of the completed feedhorn was tested on my bench, and conclusions are presented in Section VIII.

II. Working with the W2IMU dual mode feedhorn design

This dual mode feedhorn was invented by Dick Turrin, W2IMU. It was designed to cancel the electric field at the aperture boundary resulting from the TE11 and TM11 circular waveguide modes, resulting in low sidelobes, an improved impedance match and coincident E and H field phase centers[4]. The narrower bandwidth of this design is not an issue for the RF transmission modes typically used by hams.

The beamwidth depends on the output aperture diameter. Field cancellation at the aperture is obtained by setting the flare half-angle (which controls the mode amplitude ratio) and the length of the output section (for proper phase alignment)[1]. In order to better understand what is going on, I wrote an Excel spreadsheet that calculates these two quantities from the aperture diameter, using the cutoff and guide wavelengths for circular waveguide (Paul's HDL_ANT software provides these calculations automatically, I used it to verify that my spreadsheet calculations were correct)[5].

I then performed the EM simulations over a range of output apertures (each with corresponding flare angle and output section length) to determine the set corresponding to a feedhorn efficiency curve appropriate for my 32" offset dish f/D of 0.5.

III. Electromagnetic simulation software choices

A list of some EM simulation software options suitable for microwave 3D structures is shown in Table 1[6]. These packages use either the Finite Element Method (FEM), Finite Integration Technique (FIT) or Method of Moments (MoM). The purchase and rental expense fees shown for most of these software products are well out of reach of most microwave experimenters.

Table 1. Some electromagnetic simulation software packages available.

NAME	METHOD	COST	WEBSITE
Ansys HFSS	FEM, MoM	$$$ (?)	https://www.ansys.com/products/electronics/ansys-hfss
Cadence AWR	FEM	$990/mo	https://www.cadence.com/en_US/home/tools/system-analysis/rf-microwave-design.html
COMSOL	FEM	$7996/year, $15990 perpetual	https://www.comsol.com/rf-module
CST	FIT	$2000/year, $64000 ppl.	https://www.3ds.com/products-services/simulia/products/cst-studio-suite/
FEKO	FEM, MoM	$24100/yr, $75000 perpetual	https://www.altair.com/feko
Keysight PathWave W4301b	FEM	$16545/yr, $43541 perpetual	https://www.keysight.com/us/en/product/W4301B/pathwave-em-design-core-fem-ads-rfpro-ui.html
HOBBIES academic	MoM	$249 perpetual	http://www.em-hobbies.com (currently inactive)
WIPL-D, 1K unknowns	MoM	$750/year, $2150 perpetual	https://wipl-d.com/
NEC2	MoM	Free	http://www.nec2.org

Paul Wade used NEC2[7] for his W2IMU simulations in his Antenna Book. This software works well for wire antennas and simple horn structures, but I wanted to see if there is another option that offers a user interface that is easier to handle, including displaying model features in a 3D perspective to better visualize the editing process, with the ability to change key dimensions quickly for performance optimization. In addition, I had a rectangular waveguide transition structure in mind that I wanted to add, whose practicality of implementation using NEC2 was unknown.

I first purchased the HOBBIES (Higher Order Basis Based Integral Equation Solver) software, which is accompanied by a textbook[8] and website[9]. I was able to construct the full feedhorn model with it and believe that the simulation engine is very capable, but unfortunately I encountered severe stability problems within the Windows platform. In addition, the messages displayed in response to error conditions were cryptic and not useful, and obtaining technical support is problematic at this time.

I then turned to the WIPL-D (Wires, Plates and Dielectrics) software[3]. I spoke with a retired professional microwave engineer with extensive experience in EM simulation[10]. He advised me that WIPL-D uses exact integral field equations internally, vs. approximate versions that NEC2 uses. He mentioned other advantages of WIPL-D over NEC2, including much faster execution, lower memory requirements, ability to handle dielectrics and freedom from NEC2's restrictions regarding structure thicknesses and angles in its wire model paradigm.

I chose to rent WIPL-D for 1 year (the license is tied to a USB dongle, not a fixed PC). This uses a simulation engine that is very similar to that of HOBBIES, but with excellent stability and technical support in my experience. The remainder of this paper uses this software choice.

There are also several open-source and free EM simulators available, however I decided to only consider software packages with a known professional reputation with full technical support available.

IV. Highlights of WIPL-D Method of Moments calculations

A. Integral field equation[11,12]

WIPL-D uses a model for electric current densities on surfaces and calculates the corresponding electric and magnetic fields outside of them using Maxwell's equations for electromagnetism. This discussion is limited to perfect conductor surfaces in vacuum (electrical permittivity is ε_0, no dielectrics) for simplicity. Figure 1 below shows how the electric field at a point M originates from the current density **J** at a point located on an arbitrary surface S', located in a vacuum. The vectors **r** and **r'** specify the coordinate locations of M and J respectively.

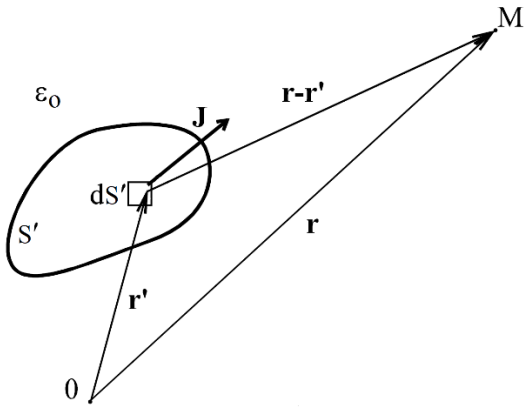

Figure 1. Electric field at point M originating from current density at a surface point.

The electric field resulting from all of the currents on the surface is obtained by integrating the (variable) current density Js and a quantity called the Green's function over the whole surface, using an Electric Field Integral Equation (EFIE) similar to the following, with the electric field vector $\mathbf{E_i}(\mathbf{r})$ on the right side:

$$\int_{S'} \mathbf{u}(\mathbf{r}) \cdot \left(\mathbf{J}_s(\mathbf{r}')g(\mathbf{r},\mathbf{r}') + \frac{1}{k^2} \operatorname{div}'_s \mathbf{J}_s(\mathbf{r}') \operatorname{grad} g(\mathbf{r},\mathbf{r}') \right) dS' = \frac{\mathbf{u}(\mathbf{r}) \cdot \mathbf{E}_i(\mathbf{r})}{j\omega\mu_0}$$

The current density Js and its derivative and also the Green's function g (and vector derivative) depend on to the vector locations **r** and **r'**. **u(r)** represents the coordinate system unit vector and μ_0 is the magnetic permeability in vacuum.

B. Method of Moments[14]

In the Method of Moments, the current density for a plate surface is modeled using a pair of algebraic polynomials, each containing increasing powers of position coordinate variables s and p. Figure 2 shows a surface patch within a plate where the current depends on these two variables.

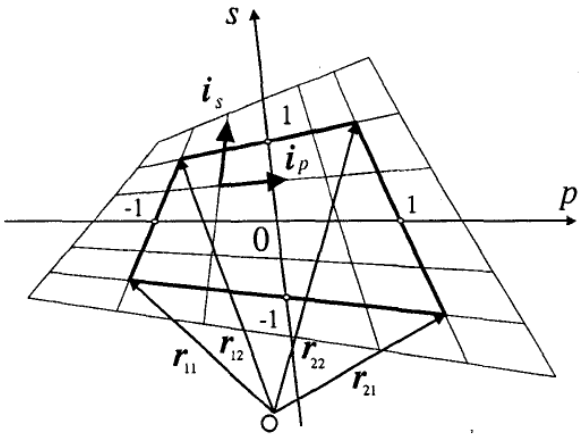

Figure 2. Surface patch coordinate system used by current density at a point.

The current density J_{ss} is then modeled as:

$$J_{ss}(p,s) = \frac{1}{e_p(s)\sin\alpha_{ps}(p,s)} \sum_{j=0}^{n_p} \left[\sum_{i=0}^{n_s} a_{ij} s^i \right] p^j \ ,$$

These polynomials are called higher order basis functions, and the objective is to determine the values of the term coefficients a_{ij}. Inserting this current density summation into the integral equation results in a set of N pairs of integral equations. By taking the inner ("dot") product of a second set of (weighting) functions with both sides of each integral equation and numerically evaluating the integrals, a system of N linear equations in N unknown coefficients is obtained. The weighting functions are the same as the basis functions (but without coefficients) in WIPL-D, following the Galerkin method. Inverting this linear algebra matrix can be performed, but more computationally efficient methods are used instead to obtain the set of coefficients.

This linear equation process enforces fundamental electromagnetic boundary conditions, such as the fact that only the normal component of the electric field (that which is perpendicular to the surface) is nonzero on the surface of a perfect conductor.

After the coefficients are determined, Maxwell's equations are used to calculate the other electromagnetic quantities of the system. A plate constructed in a WIPL-D model will contain one or more of these sets of calculations (meshing elements), such that the total number of unknowns to be solved for will be about 30 unknowns per square wavelength of plate area (the polynomial order of the basis functions increases as the plate dimension increases in units of wavelength)[15].

Calculations for wires are much simpler, which assume that only the component of the current flowing down the length of the wire is nonzero (called the thin-wire approximation). About ten unknowns per wavelength of length will be needed in this case.

WIPL-D derives meshing elements from the geometric features of the model as it is constructed, as opposed to performing a separate meshing operation after the model is completed as is done with some other EM simulation software packages. The meshing element density can be explicitly increased by subdivision of model sections, as will be shown later.

V. Waveguide termination as a WIPL-D example

A. Constructing the model

A simple waveguide termination serves to introduce the WIPL application. The structure consists of a wedge-shaped piece of partially conducting dielectric material[16] that absorbs incoming 47 GHz RF energy arriving at the end of a length of WR22 waveguide, which is excited by a probe wire located approximately one quarter wavelength ahead of a back short plate. The dielectric parameters were set to a relative electric permittivity of 1.0, a relative magnetic permeability of 1.0, and a conductivity of 5.0 Siemens/m[17]. The conductivity of all plates and wires was set to a real-world value of 19 Siemens/m[18]. Figure 3 shows the completed model.

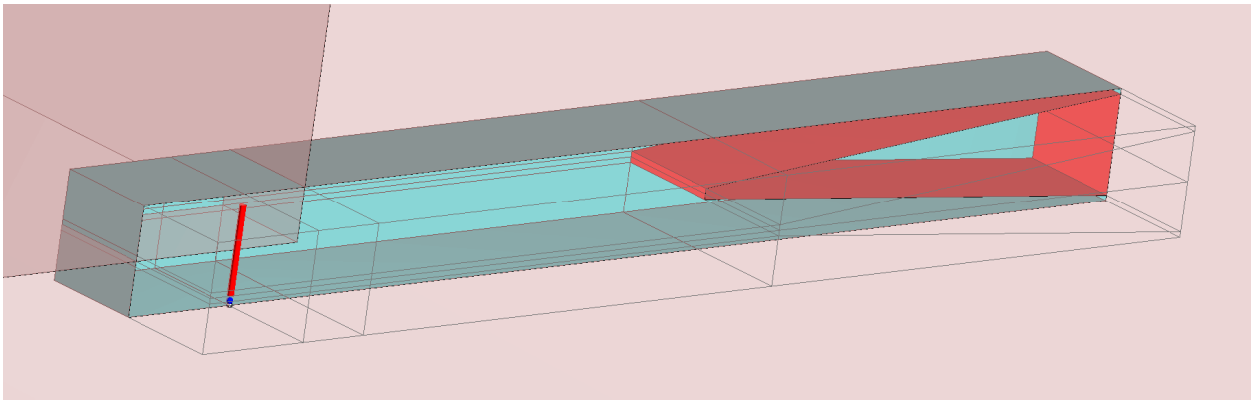

Figure 3. Dielectric termination model.

Like many EM simulation programs, WIPL-D takes advantage of symmetry in the object being modeled in order to reduce the number of meshing elements required (the economy version of the software I'm using has a limitation of 1000 unknown parameters). Only one half of the termination model need actually be constructed to obtain the behavior of the full structure, this is highlighted by the X-Z symmetry plane (Y-axis symmetry) in the figure. Note the vertical probe wire (in X direction) with the generator at the base of it.

B. Optimizing the probe and backshort length for minimum return loss

The termination return loss frequency response (S11) obtained is shown in Figure 4, in which the backshort distance was varied to minimize S11 (the probe wire height primarily governs bandwidth and was set to 80% of the waveguide narrower dimension). WIPL-D's sweep tool was used for this, as shown in Figure 5 where the backshort distance was swept with the frequency and all other parameters held constant at 47088 MHz. The backshort distance was optimized at 1.08 x the waveguide narrower dimension.

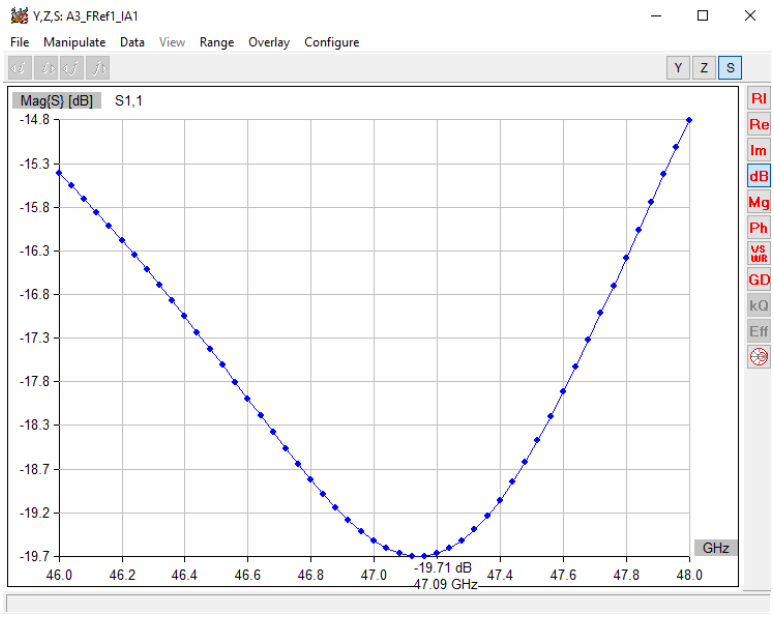

Figure 4. Optimized return loss at probe feedpoint.

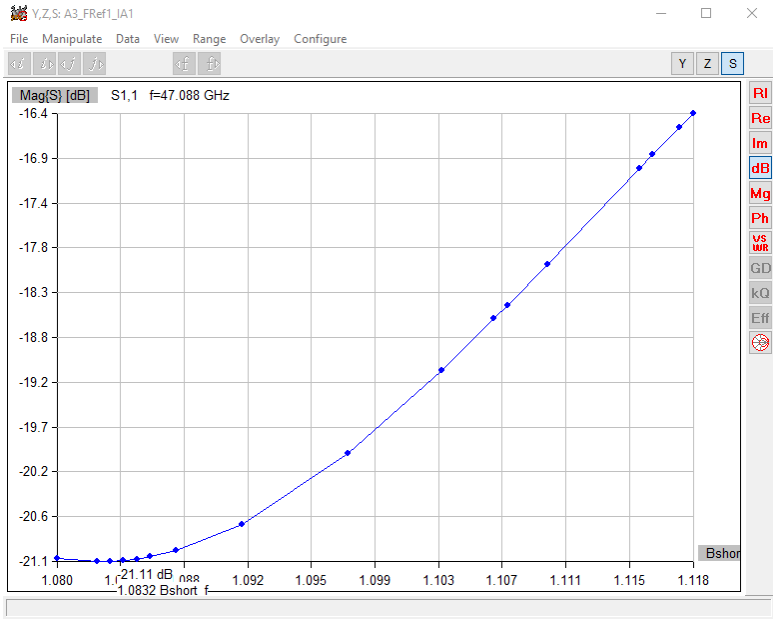

Figure 5. Return loss vs. relative backshort distance at 47.088 GHz.

VI. W2IMU feedhorn structure

I knew that simulating the feedhorn design for the purpose of evaluating its return loss and radiation pattern efficiency would require excitation by a probe wire into a section of rectangular waveguide (WR22) connected to the feedhorn input. Figure 5 shows the feedhorn model.

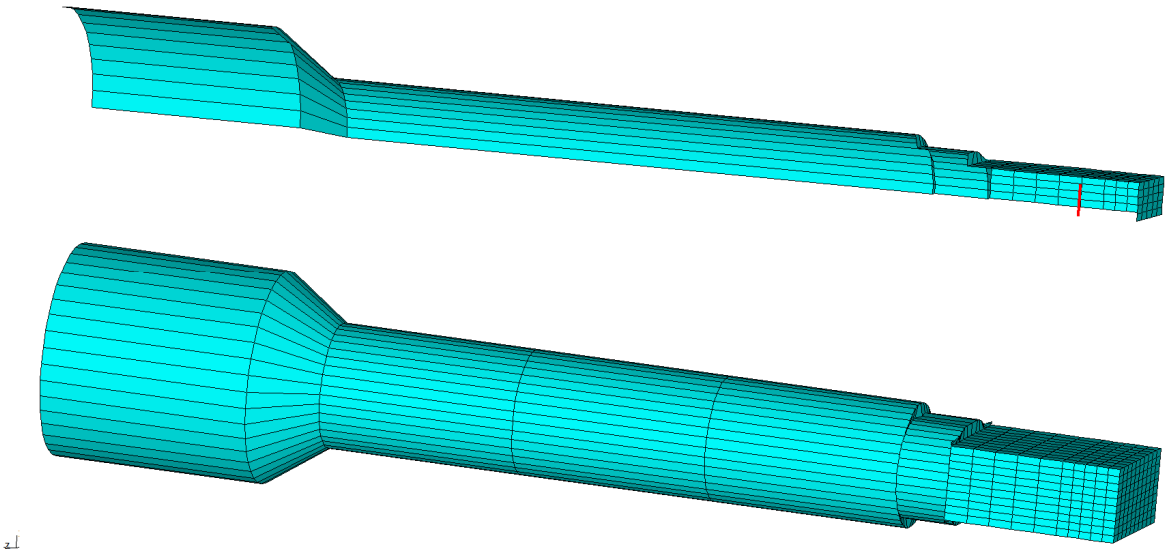

Figure 5. W2IMU feedhorn model (quadrant and full views).

Even though a wire feed is not used in the physical feedhorn design, the WIPL-D software requires an excitation generator to operate on a wire (the software supports direct EM wave excitation, but only for scattering analysis problems). The de-embedding technique removes the effect of the probe and rectangular waveguide from the return loss calculation (to be discussed in the next section). De-embedding is not used for the radiation pattern calculations.

A. Principal model components

The model consists of three parts:

1. The W2IMU dual mode horn structure sized for 47 GHz, consisting of an output aperture section, a reducer neck, and a section of circular waveguide. As a starting point, I set the output aperture to 1.30 (free space) wavelengths, with the output section length and flare half-angle set according to my spreadsheet as described previously. I used the standard Q band circular waveguide I.D. of 0.188 inches, with G0IVA's dimension for the circular waveguide length.
2. An oval-shaped transition section, nominally one quarter wavelength long. Its width and height were sized to fall roughly in between the circular waveguide diameter and the width and height of WR22 rectangular waveguide. I found Paul Wade's use of this transition section for the 24/10 GHz dual band machined feedhorn[19] discussed in his website to be very helpful.
3. The same rectangular waveguide and probe structure as used for the termination model, except that the excitation probe is now a centrally positioned dipole instead of a monopole protruding from the waveguide wall.

Note again that the rectangular waveguide and probe are just simulation devices and are not present in the actual feedhorn. Also, I decided to have the oval transition section fabricated as a physically

separate plate, attached to the circular feedhorn input, in order to compare the return loss with and without the use of it.

B. Model construction

There are three principal model construction steps:

1. Definition of symbols (variables) that define dimensions and coordinate values.
2. Creation of the nodes that define the model coordinate points, these are specified by X, Y and Z numbers or variables from the symbol table.
3. Creation of the plates, each of which are defined by 4 nodes.

For construction of radially-symmetric bodies, WIPL-D has a template called a Body of Revolution, which uses the cylindrical coordinate system. This was used to construct the dual mode feedhorn proper as listed in Part 1 above. For the reducer neck as an example, the two different radii are specified along with a subdivision parameter n. The model shows n as having a value of 10 divisions along the perimeter of the quadrant (including the rectangular waveguide feed), but this can be varied to increase or decrease the meshing element density as desired.

The reason for the dipole feed was to enable symmetry along the X axis, in addition to the Y-axis symmetry employed in the termination model. This requires only one physically constructed quadrant (as seen in the model view above), further reducing the number of meshing unknowns needed by about a factor of two. Note that if this feedhorn were constructed with a real dipole feed, the return loss would be poor, due to the smaller waveguide dimension not physically accommodating a full half-wavelength wire. However, this does not impede the embedding functionality for simulating the return loss in response to RF energy entering the feedhorn input port.

The oval transition section consists of two 90 degree arcs, each displaced from the center feedhorn axis in the +- Y direction.

C. Use of de-embedding

WIPL-D implements de-embedding by means of a separate Feed structure (Figure 6) which in this case simply duplicates the section of rectangular waveguide and probe structure up to the input port of the physical feedhorn proper (where the oval transition begins). The simulation is first run using the main feedhorn model without de-embedding. The Feed structure is simulated by itself next. Finally, the main model output file is recalculated (using previously stored data) with de-embedding enabled, which effectively moves the reference plane from the probe wire location to the feedhorn input port.

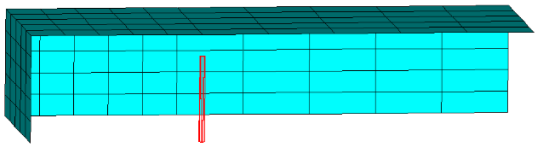

Figure 6. Network feed structure.

VII. Simulating and testing the feedhorn

A. Simulation format

The WIPL-D software was used to obtain the return loss (S11) and the E and H field polar gain patterns. Field values can be calculated at either infinity or at a finite distance, I chose the latter option and set it to my offset dish focal length.

Paul Wade has two software programs that calculate the feedhorn efficiency vs. f/D, both work by integrating the portion of the radiation pattern intercepted by my 32" offset dish. I used his Phasepat program[20], using an Excel macro to resort the magnitude and phase data from WIPL-D's 2D radiation pattern output file into the required Phasepat input format.

Phasepat adds wavefront phase information to the gain input data for a more accurate efficiency result. This requires knowledge of the phase center location, which is defined as the coordinate location within the feedhorn structure from which all the energy will strike the dish with the same phase, as if that coordinate location were a point source. This should coincide with the parabolic dish focal point. In fact, the optimum phase center can be found by varying the phase center Z-axis distance (relative to the output aperture plane) to maximize Phasepat's efficiency result for a given f/D[21]. To reduce calculation complexity, I selected two phase center candidates to use to see the effect of varying the efficiency peak location vs. f/D.

I obtained the phase center #1 value by first graphing WIPL-D's E field and H field phase components of the 2D radiation pattern, then I varied the radiation pattern origin distance (from the coordinate system origin) in WIPL-D. I selected an origin distance that caused the average relative phase deviation from its on-axis value to be minimized for both E field and H field components, with emphasis on the angular region close to the on-axis direction. As expected, this new origin is close to the output aperture.

Phasepat has an option for selecting the best phase center value over a specified range from an input phase data file. I used this tool to obtain phase center value #2, using WIPL-D's phase data taken with value #1 above.

I used Phasepat to obtain the feedhorn efficiency graphs at 1.30, 1.28 and 1.277 wavelengths output aperture, for both phase center values, to evaluate the peak location behavior vs. f/D for purposes of choosing a set of dimensions for actual fabrication.

B.Simulation results (rectangular waveguide transition section optimization)

The oval transition width and height were set to values midway between the pair of WR22 waveguide dimensions and the circular waveguide diameter, and the thickness was set to a nominal 0.0875 inches.

I used the sweep tool to vary the transition section thickness about the nominal quarter wavelength (with the frequency and all other parameters held constant at 47088 MHz). The optimum dimension was established at 0.081 inches for a return loss of – 40.3 dB. I decided not to bother with varying the transition width or height.

Figure 7 shows the optimized return loss vs. frequency for a 1.30 wavelength output aperture.

I then effectively removed the transition entirely by setting the transition thickness to a negligibly small value with the two arcs merging into a circle with the same diameter as the circular waveguide. Figure 8 shows the results for nominal and near-zero thicknesses.

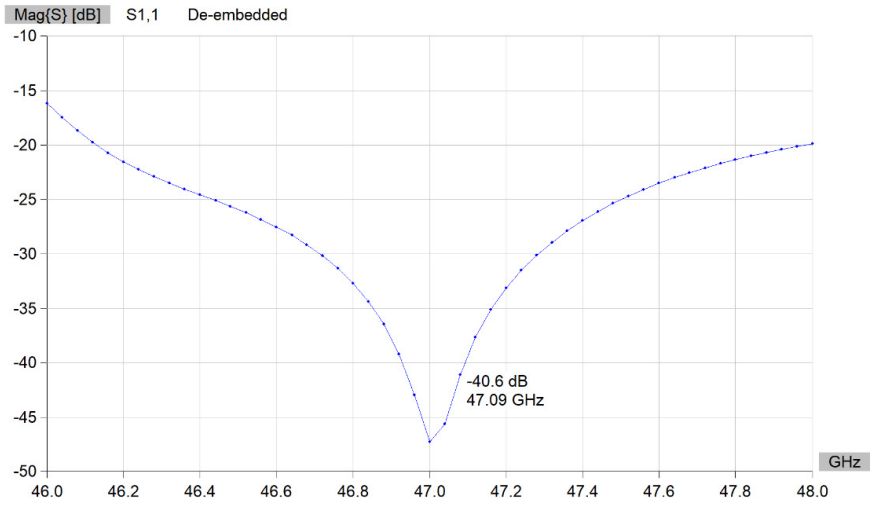

Figure 7. Return loss vs. frequency with optimized transition thickness at 1.30 wl.

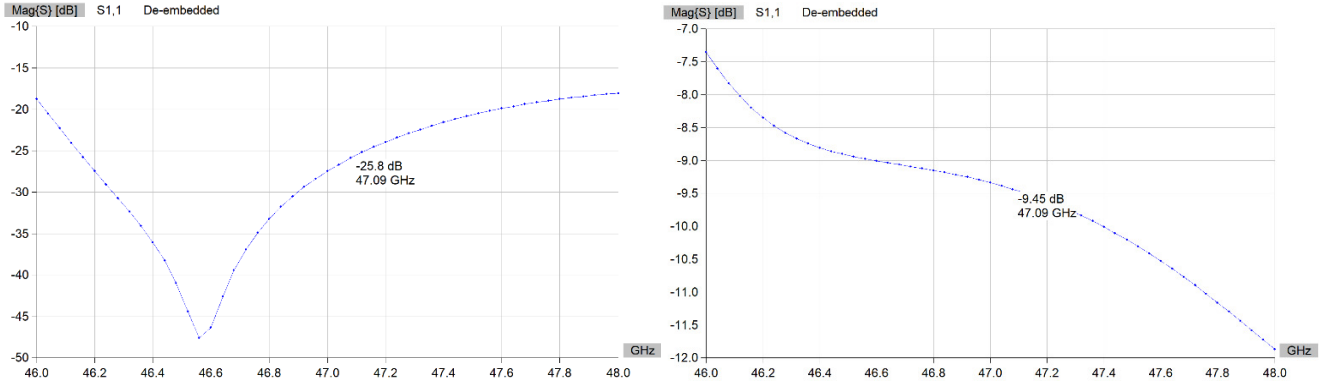

Figure 8. Return loss vs. frequency for nominal thickness (L) and near-zero thickness (R) at 1.30 wl.

C.Simulation results (feedhorn efficiency)

Starting with the phase data first, I obtained WIPL-D's E-field and H-field phase components of the 2D radiation pattern for the 1.30 wavelength feedhorn dimensions, and iterated this process over a range of WIPL-D's radiation pattern origin settings. WIPL-D allows the 2D pattern calculation distance to be set at either infinity or at a finite distance, which I set to be 20 inches to match my dish focal length.

Figure 9 shows the finite distance results obtained, with the pattern origin set for the best phase center, judged to be 0.224 wavelengths outside of the aperture plane (phase center #1). For reference, repeating this process at infinity resulted in the best phase center to be about 0.017 wavelengths outside the aperture plane.

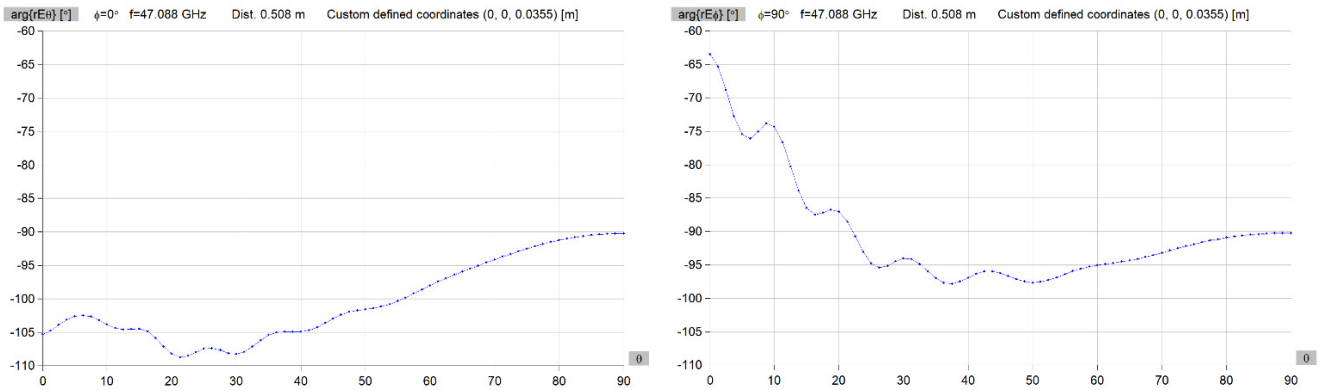

Figure 9. E field (L) and H field (R) radiated phase pattern components with adjusted radiation pattern origin, for 1.30 wavelength feedhorn dimensions and with phase center #1.

I next obtained E and H field gain and phase data for 1.30, 1.28 and 1.277 wavelengths output aperture, calculated at my dish focal point, with WIPL-D's radiation origin set for phase center value #1. The data were exported to the Phasepat program as described above. Its output graphs for 1.30 and 1.28 wavelengths are shown in Figure 10. Gain has been normalized to the on-axis value, and I used Adobe Photoshop to flatten the EPS output files for display. Peak efficiency was about 77 % at 0.58 f/D for 1.30 wavelengths and about 73 % at 0.57 f/D for 1.28 wavelengths.

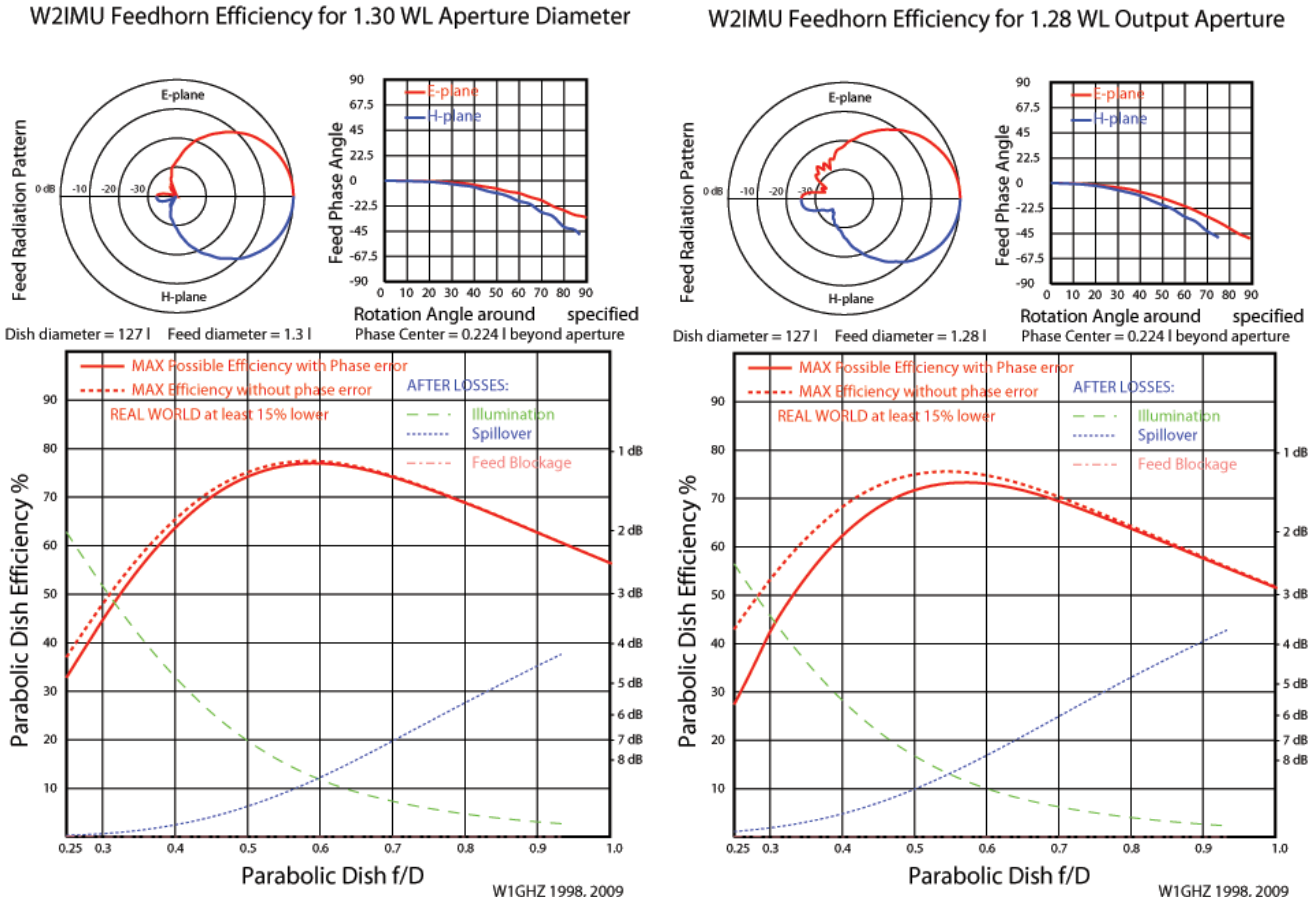

Figure 10. Gain and efficiency plots for 1.30 wl (L) and 1.28 wl (R) aperture with phase center #1.

WIPL-D's phase data taken with the 0.224 wavelength phase center value was then used to obtain Phasepat's new suggested phase center value of 0.0885 wavelengths outside of the aperture, and a new set of gain and phase data were obtained for the three output apertures. Figure 11 shows the results for the 1.30 and 1.28 wavelength parameter sets.

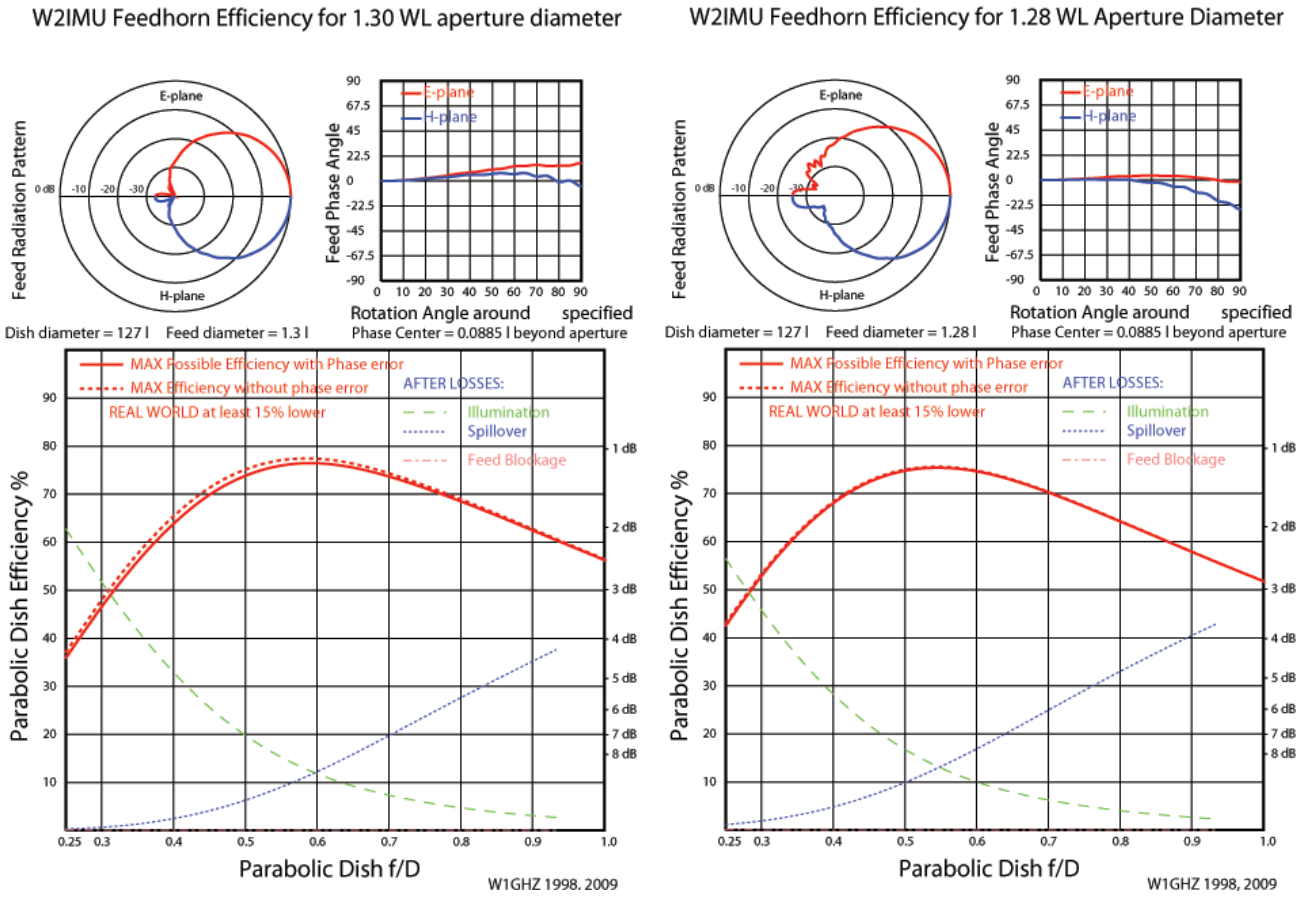

Figure 11. Gain and efficiency plots for 1.30 wl (L) and 1.28 wl (R) aperture with phase center #2.

For reference, the E and H field absolute gain patterns from WIPL-D at 1.30 wavelengths are shown in Figure 12.

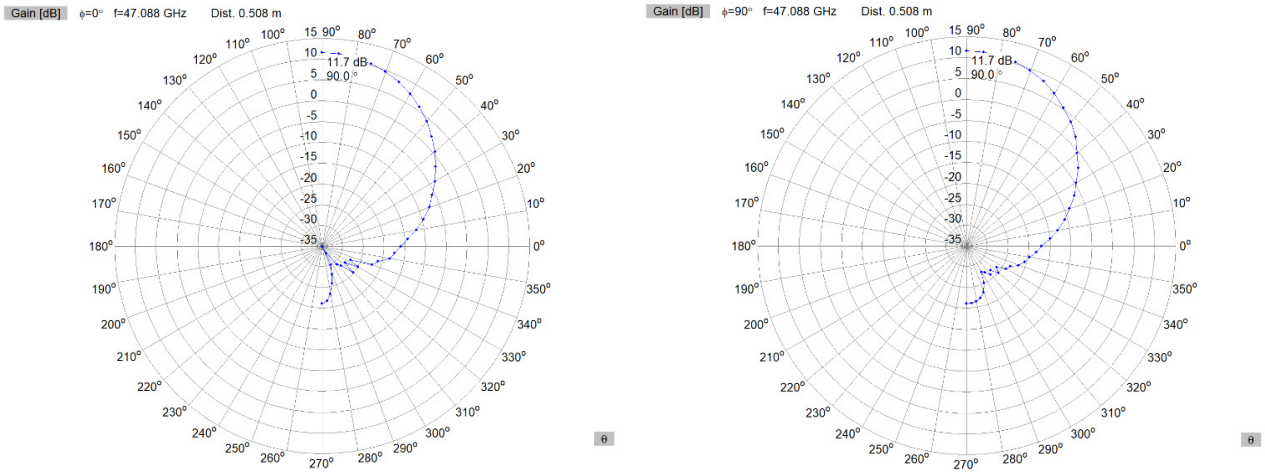

Figure 12. E field (L, 11 dB absolute on-axis gain) and H field (R, 11 dB gain) at 1.30 wavelengths.

These plots warrant further discussion. My original intent was to simply shift the efficiency peak down closer to 0.5 f/D, which did indeed occur. However, the new plots show that the peak efficiency value also decreased. This is noticeable with phase center #1, even more so for the curves with phase error included.

Selecting phase center 2 results in a much smaller peak efficiency change with decreasing aperture diameter. In addition, the effect of phase error is much smaller. The efficiency (at 0.5 f/D) for 1.28 wavelengths is slightly higher than the efficiency for 1.30 wl, for the same f/D value, about 75 % at 0.5 f/D for 1.28 wl. The E and H gain patterns became increasingly asymmetric as the output aperture was decreased. The data for the 1.277 wavelength aperture continue the same trends in peak efficiency, effects of phase error and pattern asymmetry (not shown).

As a check on the meshing resolution used for the simulations, I decreased the "n" parameter from 10 to 6 and re-ran the return loss and efficiency plots. Doing this decreases the accuracy of curved surface rendering in the model, but also decreases the number of calculation unknowns required, as well as decreasing the simulation run time. Figure 13 shows the decreased meshing density.

The leftward curve shift, peak efficiency decrease and changed H-field plot shape (for the smaller output apertures) seen above was also evident with the lower meshing density (not shown). The return loss at 47.088 GHz with the lower n value was -41.1 dB (vs. -40.3 dB with the higher n value).

I had been using Feedpatt[22] for the efficiency calculations earlier in this project, and I decided to adopt the 1.30 wl parameter set for fabricating my feedhorn for best performance with my dish based on those results, which did not include phase error. The Phasepat results would seem to indicate that a 1.28 wavelength aperture would have performed well also.

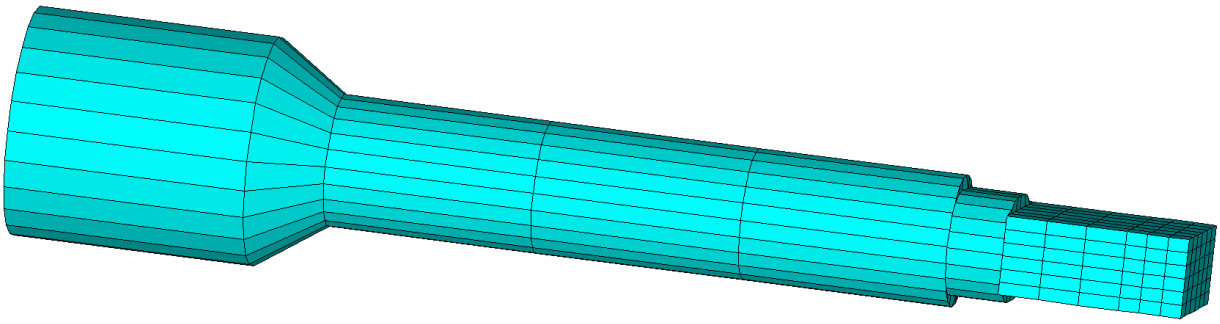

Figure 13. n parameter decreased from 10 to 6 to decrease meshing density.

Table 2 shows a summary comparison of the feedhorn efficiency and peak f/D at 1.30 wavelengths aperture obtained using WIPL-D and Phasepat at phase center #2, vs. what was calculated in Paul's examination of the G0IVA model.

Table 2. Comparison of peak efficiencies at peak f/D for 1.30 wavelength output aperture.

CALCULATION SOURCE	PEAK EFFICIENCY (%)	PEAK f/D RATIO
G0IVA (ANTENNA BOOK ONLINE)	77.0	0.52
WIPL-D	76.5	0.58

C. Finished unit testing

The feedhorn was fabricated at a machine shop according to the optimized dimensions shown in Figure 14.

Varying the transition thickness +- 2 mils away from the optimum value caused the simulated return loss to drop several dB but still remain acceptable, so I specified +- 0.001 inch machining tolerance for the most critical feedhorn dimensions.

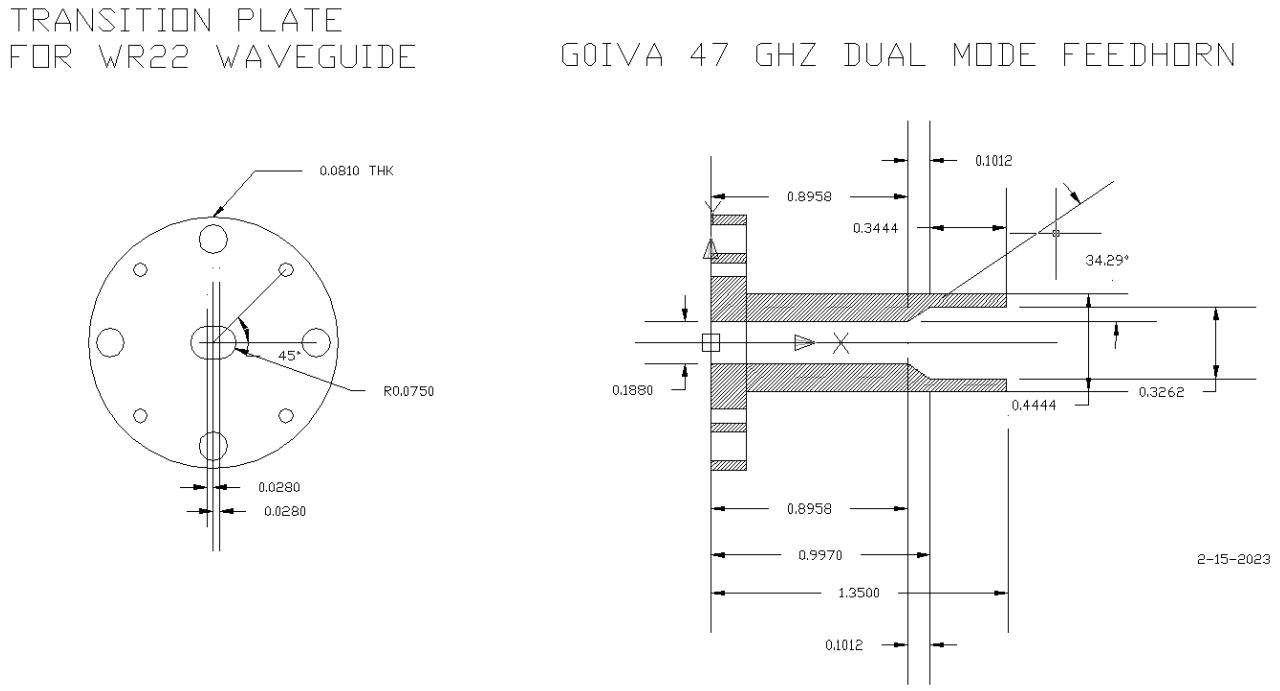

Figure 14. Fabrication drawing for the optimized feedhorn and transition plate.

I measured the return loss on my test bench using a synthesized source, multiplier chain, directional coupler and harmonic mixer on my spectrum analyzer. The S11 result was -23.0 dB at 47.088 GHz with the oval transition plate included, likely limited by measurement accuracy (vs. -40 dB for the optimized simulation result), and -8.8 dB with the transition plate removed. Figure 15 shows the fabricated feedhorn and bench test setup.

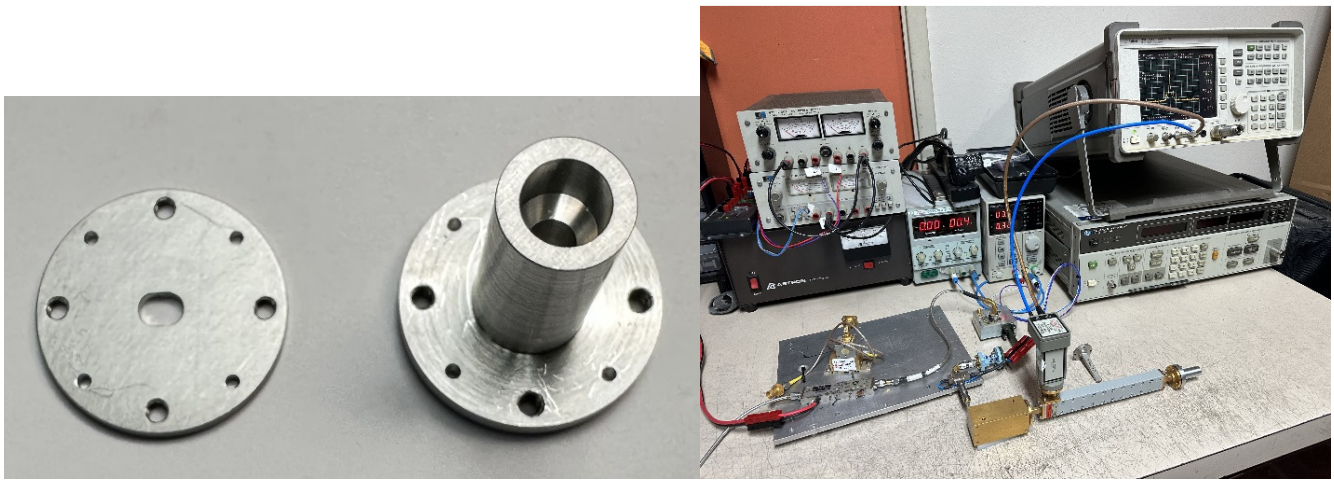

Figure 15. Fabricated feedhorn and return loss test setup.

VIII. Conclusions

I established a suitable set of dimensions for fabricating my feedhorn, and I hope that my application of WIPL-D to validate its performance for my dish will be of practical interest to microwave hams. Trying out varying feedhorn output aperture sizes was invaluable in my decision to stay with the original 1.3 wavelength design for my 0.5 f/D dish application. The best phase center could have likely been refined for further improvements at smaller apertures by evaluating more trial values if time permitted. The 1000 unknown limit for this version of WIPL-D proved to be sufficient for accommodating this feedhorn's structural complexity, and I look forward to more projects that leverage WIPL-D's capability in the future.

I wish to thank Paul Wade for his invaluable Antenna Book Online resource (and personal advice) towards getting my effort going in the right direction. The technical support folks at WIPL-D were very helpful in bringing me up to speed on their software and in getting an idea of how the method of moments works. Also many thanks to Steve Stearns for his assistance with my earlier struggles with the HOBBIES software and pointing me to WIPL-D, and to Mike Lavelle K6ML for reviewing a draft.

IX. REFERENCES

[1] Paul Wade, W1GHZ, "Part 1 – Practical Antennas" in *The W1GHz Online Microwave Antenna Book*, Dual-Mode Feeds, W2IMU dual-mode feed, 1999, http://www.w1ghz.org/antbook/ch6_5-1.pdf, 6.5.1.

[2] Paul Wade, W1GHZ, "Part 1 – Practical Antennas" in *The W1GHz Online Microwave Antenna Book*, Dual-Mode Feeds, W2IMU dual-mode feed examples, 1999. http://www.w1ghz.org/antbook/ch6_5-1.pdf, 6.5.2.

[3] WIPL-D Pro software, Gandijeva 7 apt 32, 11073 Belgrade, Serbia, Europe. https://wipl-d.com/

[4] R. H. Turrin, "Dual Mode Small-Aperture Antennas" in *IEEE Transactions on Antennas and Propagation*, AP-15, March 1967, pp. 307-308, 1967.

[5] Paul Wade, W1GHZ, HDL_Ant software, "Software for Microwaves" website, http://www.w1ghz.org/10g/software.htm.

[6] "Comparison of EM simulation software" from Wikipedia, *http://en.wikipedia.org/wiki/Comparison_of_EM_simulation_software*

[7] Numerical Electromagnetics Code software, repository website, http://www.nec2.org.

[8] Y. Zhang, T. Sarkar, X. Zhao et. al., Higher Order Basis Based Integral Equation Solver (HOBBIES), 1st ed. Hoboken NJ: Wiley Publishing, 2012.

[9] http://www.em-hobbies.com (currently inactive).

[10] Steve Stearns, K6OIK, personal communication, November 2022. He is a retired Technical Fellow at Northrup Grumman. List of his technical articles for hams: https://www.fars.k6ya.org/docs/

[11] T. Sarkar, A. Djordjevic and B. Kolundzija, "Method of moments" in *Method of Moments Applied to Antennas*, online PDF, 2000, pp. 8-12. Believed to have same content as in reference [13] below.

[12] T. Sarkar, A. Djordjevic and B. Kolundzija, "Antenna analysis" in *Method of Moments Applied to Antennas*, online PDF, 2000, pp. 22-26. Believed to have same content as in reference [13] below.

[13] T. Sarkar, A. Djordjevic and B. Kolundzija, "Method of Moments Applied to Antennas" in *Handbook of Antennas in Wireless Communications*, 1st ed. Boca Raton FL: CRC Press, 2002, ch. 8.

[14] B. Kolundzija, J. Ognjanovic, T. Sarkar et. al., "WIPL: A Program for Electromagnetic Modeling of Composite-Wire and Plate Structures" in IEEE Antennas and Propagation Magazine, Vol. 38, No. 1, pp. 77-78, 1996.

[15] B. Kolundzija, "5 Generations of Higher Order Bases: General Approach for Highly Accurate and Efficient EM Modeling", WIPL-D resources page video, 27 May 2021.

[16] R. Collin, "Passive Microwave Devices" in Foundations for Microwave Engineering, 2nd ed. Hoboken NJ: Wiley-Interscience, 2001, ch. 6, pp. 394-395.

[17] From a research paper found online, origin unfortunately lost.

[18] WIPL-D technical support guidance, December 2022.

[19] Paul Wade, W1GHZ, "Improving the Dual-band 10 & 24 GHz Feedhorn for Offset Dishes", in his website, 2004.
http://www. http://www.w1ghz.org/new/dualband_feedhorn.pdf

[20] Paul Wade, W1GHZ, Phasepat software, "Software for Microwaves" website, http://www.w1ghz.org/10g/software.htm.

[21] Paul Wade, W1GHZ, "Part 3 – Computer Analysis of Antennas" in *The W1GHz Online Microwave Antenna Book*, Pattern Calculation and Phase Analysis, 1999, http://www.w1ghz.org/antbook/chap12.pdf, 12.5

[22] Paul Wade, W1GHZ, Feedpatt software, "Software for Microwaves" website, http://www.w1ghz.org/10g/software.htm.